Electronic Supplementary Material (ESI) for Journal of Materials Chemistry C.

Vapor Triggered fluorescent color changes among solvates of Emodin

Meiqi Li, Qi Zhang, Hongyan He, Jian-Rong Wang and Xuefeng Mei*

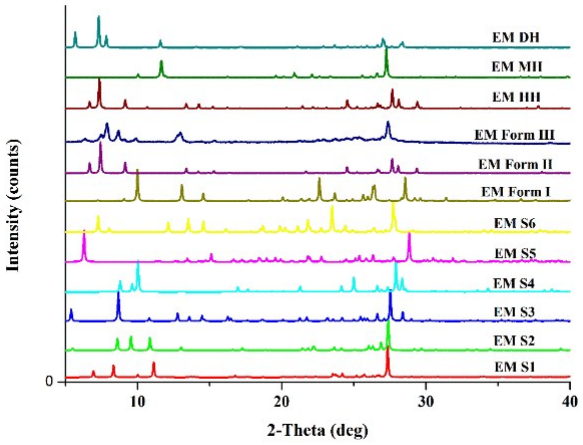

Figure S1. XRPD comparison of EM solvates, hydrates and polymorphs.

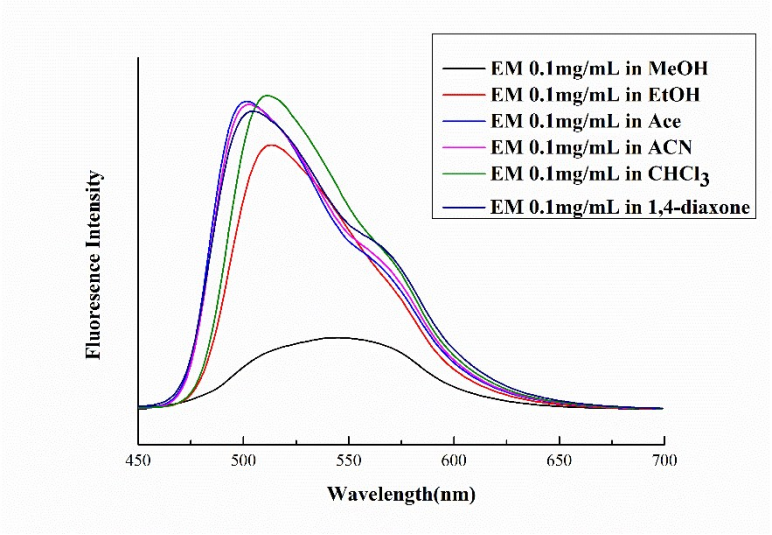

Figure S2. Fluorescent spetra of EM in different solvent with a concentration of 0.1 mg/mL.

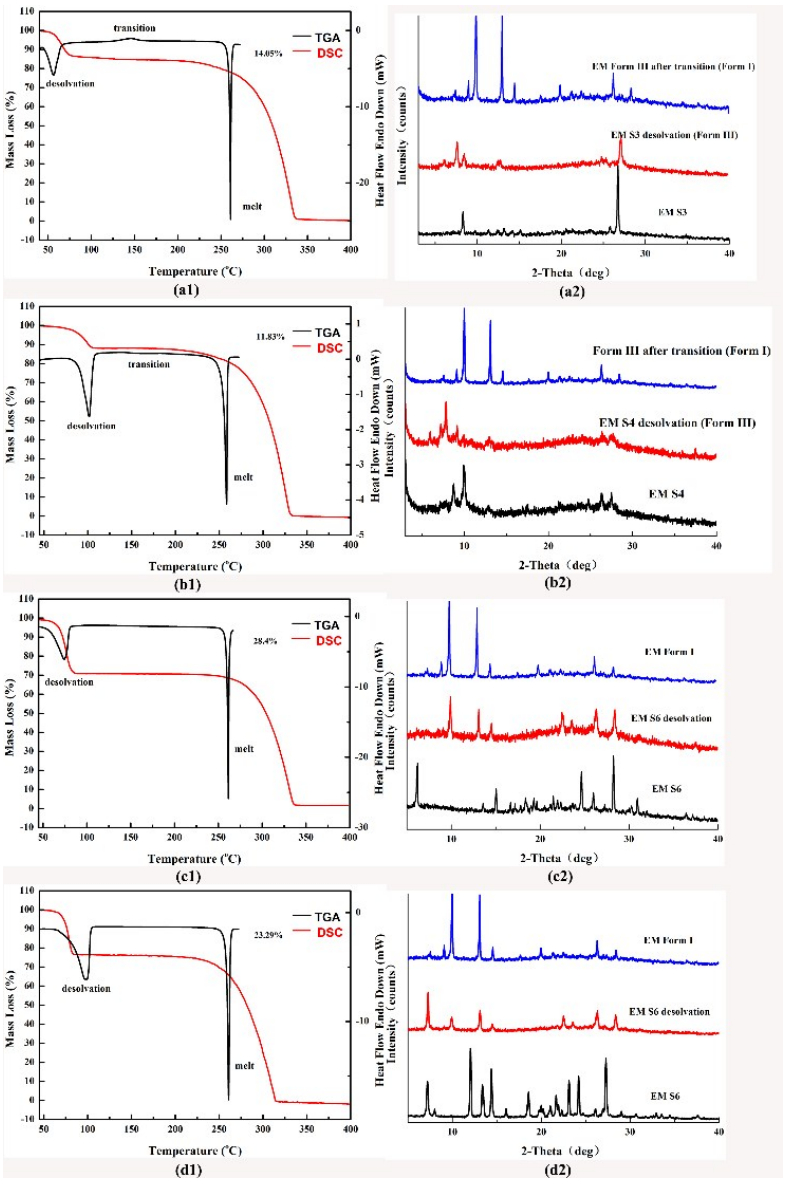

Figure S3. TGA, DSC diagrams and desolvation XRPD patterns of EM solvates. (a1) TGA & DSC diagram of S3, (a2) desolvation XRPD of S3, (b1) TGA & DSC diagram of S4, (b2) desolvation XRPD of S4, (c1) TGA & DSC diagram of S5, (c2) desolvation XRPD of S5, (d1) TGA & DSC diagram of S6, (d2) desolvation XRPD of S6.

Table S1. Thermal data (TGA and DSC) for EM solvates

Guest molecule	Methanol (S1)	Ethanol (S2)	Acetone (S3)	Acetonitrile (S4)	Chloroform (S5)	1,4-diaxone (S6)
Properties	Channel	Channel	Isolated	Channel	Channel	Channel
Calcd weight loss (%)	10.6	14.6	17.7	13.2	30.6	24.58
Obsd weight loss in TGA (%)	8.2	13.5	14.1	11.8	28.4	23.3
Guest loss Ton in DSC (oC)	79.8	69.5	46.9	90.5	58.63	81.2
Solvent boiling point (oC)	64.7	78.3	56.5	81.5	61.3	88.1
ΔH for guest loss (J g-1)	145.5	127.2	69.8	100.1	100.3	151.9

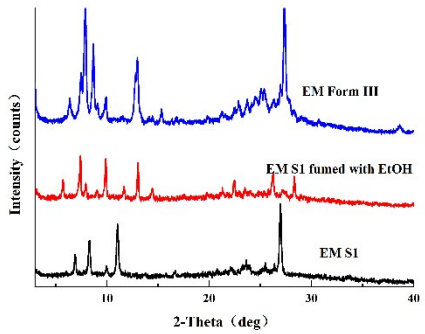

(a)

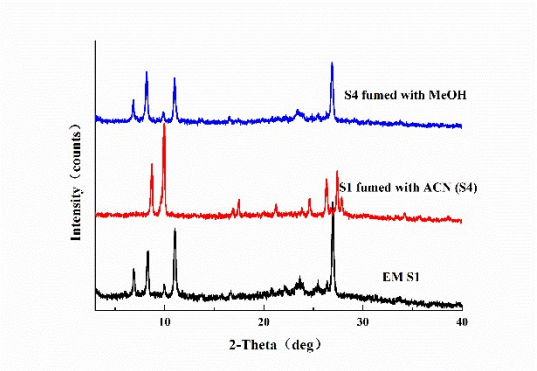

(b)

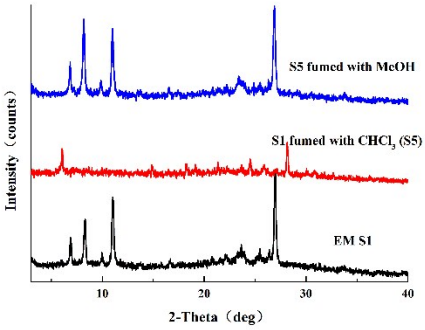
S5 fumed with MeOH
S1 fumed with CHCl3 (S5)
EM S1
Intensity（counts）
2-Theta（deg）
10
20
30
40

(c)

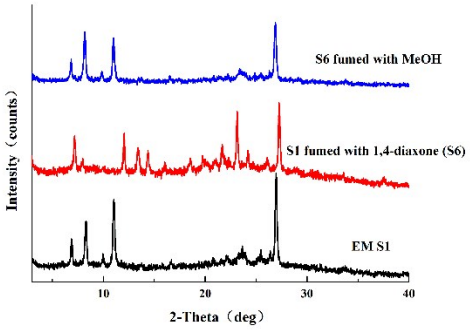
S6 fumed with MeOH
S1 fumed with 1,4-diaxone (S6)
EM S1
Intensity（counts）
2-Theta（deg）
10
20
30
40

(d)

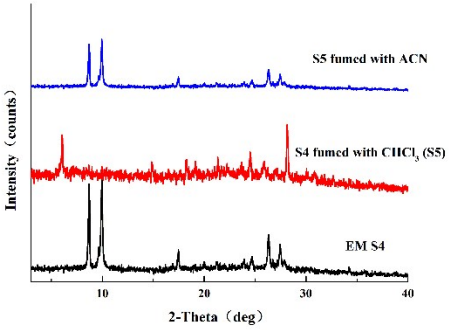
S5 fumed with ACN
S4 fumed with CHCl3 (S5)
EM S4
Intensity（counts）
2-Theta（deg）
10
20
30
40

(e)

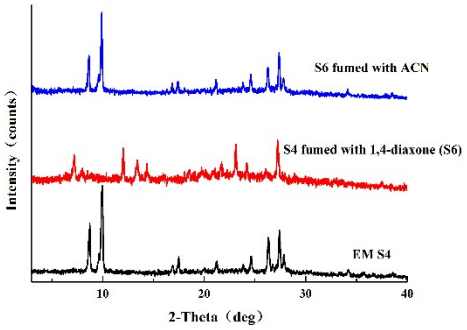
S6 fumed with ACN
S4 fumed with 1,4-diaxone (S6)
EM S4
Intensity（counts）
2-Theta（deg）
10
20
30
40

(f)

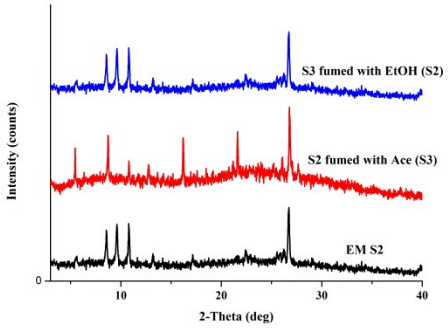
S3 fumed with EtOH (S2)
S2 fumed with Ace (S3)
EM S2
Intensity (counts)
2-Theta (deg)
0
10
20
30
40

(g)

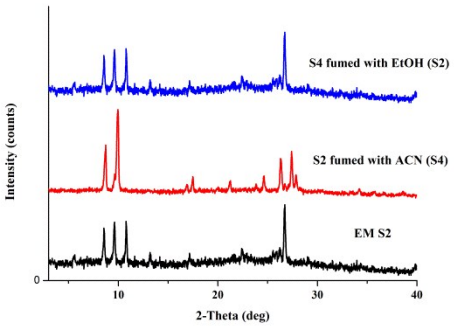
S4 fumed with EtOH (S2)
S2 fumed with ACN (S4)
EM S2
Intensity (counts)
2-Theta (deg)
0
10
20
30
40

(h)

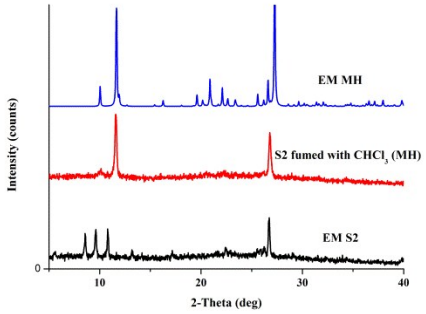

(i)

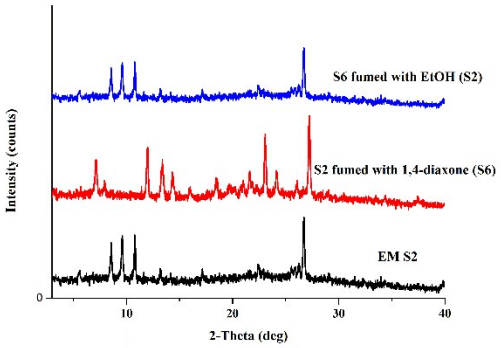

(j)

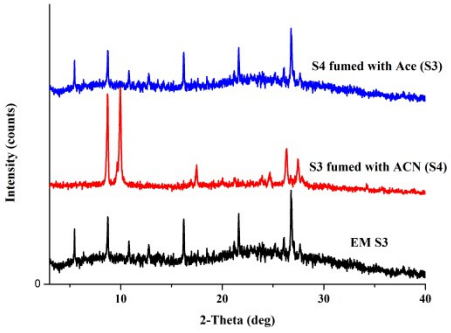

(k)

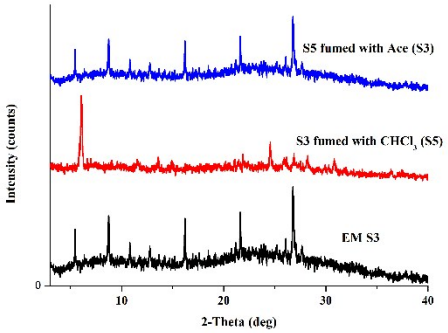

(l)

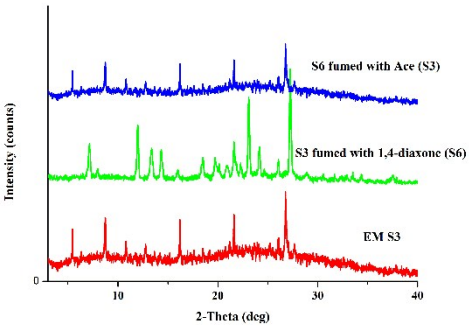

(m)

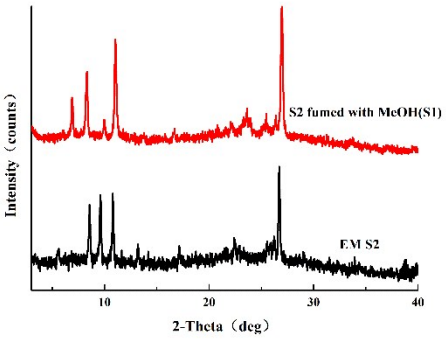

(n)

Figure S4. XRPD patterns of each combination. (a) S1-S2, (b) S1-S4, (c) S1-S5, (d) S1-S6, (e) S4-S5, (f) S4-S6, (g) S2-S3, (h) S2-S4, (i) S2-MH, (j) S2-S6, (k) S3-S4, (l) S3-S5, (m) S3-S6,(n) S2-S1

Table S2. Organic vapor mediated transition combinations of EM solvates.

organic vapor	Methanol(MeOH)	Ethanol(EtOH)	Acetone(Ace)	Acetonitrile(ACN)	Chloroform($CHCl_3$)	1,4-diaxone
S1		Form III(Figure.S3a)	Not conducted	S4(Figure.S3b)	S5(Figure.S3c)	S6(Figure.S3d)
S2	S1(Figure.S3n)		S3(Figure.S3g)	S4(Figure.S3h)	MH(Figure.S3i)	S6(Figure.S3j)
S3	Not conducted	S2(Figure.S3g)		S4(Figure.S3k)	S5(Figure.S3l)	S6(Figure.S3m)
S4	S1(Figure.S3b)	S2(Figure.S3h)	S3(Figure.S3k)		S5(Figure.S3e)	S6(Figure.S3f)
S5	S1(Figure.S3c)	S2(Figure.S3i)	S3(Figure.S3l)	S4(Figure.S3e)		Not conducted
S6	S1(Figure.S3d)	S2(Figure.S3j)	S3(Figure.S3m)	S4(Figure.S3f)	Not conducted	

"not conducted": S1-S3 and S5-S6 presents almost the same fluorecent color, thus the fluorescent color and relative solid-state transitions of S1-S3 and S5-S6 were not conducted.

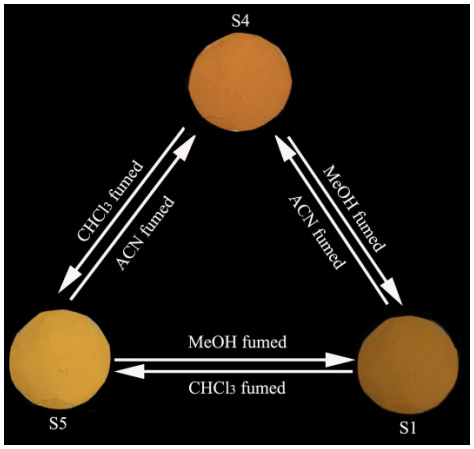

Figure S5. Vapochromic phenomena under 365 nm UV irradiation and reversible transition relationships among EM solvates (S1, S4 and S5).

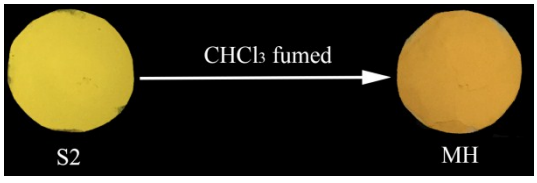

Figure S6. Vapochromic phenomena of S2 filter paper under 365 nm UV irradiation.

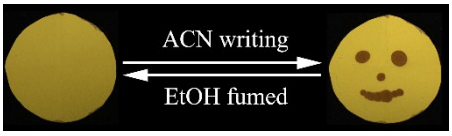

(a)

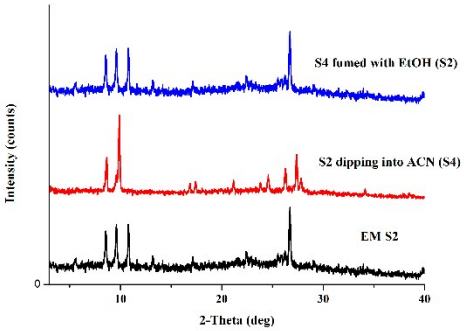

(b)

Figure S7. (a) Photographs of EM cast filter paper revealed a writing-erasing process under 365 nm UV irradiation. (b) XRPD patterns of EM S2 after dipping into acetonitrile solvent and subsequently exposing to ethanol vapor.

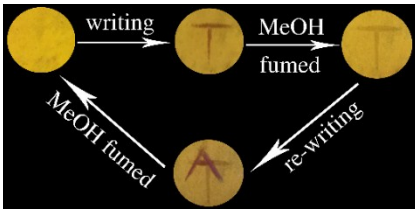

(a)

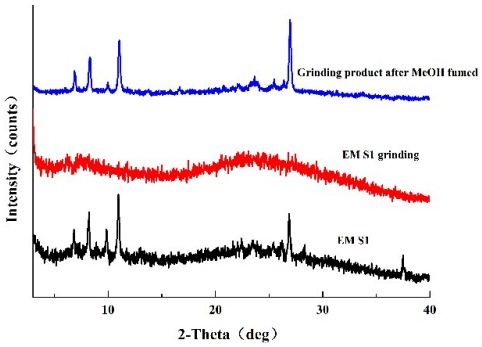

(b)

Figure S8. (a) Photographs of reversible fluorescent color changes in the writing paper made by S1. (b) XRPD patterns of S1 powder under mechanical milling and vapor treatment.

Table S3. Unit Cell Comparison for the solvates of EM

	S1	S2	S3	S4	S5	S6
Formula	$C_{15}H_{10}O_5$ CH_4O	$C_{15}H_{10}O_5$ C_2H_6O	$C_{15}H_{10}O_5$ C_3H_6O	$C_{15}H_{10}O_5$ C_2H_3N	$C_{15}H_{10}O_5$ $CHCl_3$	$C_{15}H_{10}O_5$ $C_4H_8O_2$
Crystal system	monoclinic	triclinic	monoclinic	monoclinic	triclinic	triclinic
Space group	P 2_1/n	P -1	P 2_1/c	P 2_1	P -1	P -1
Temperature (K)	100(2)	170(2)	100(2)	170(2)	170(2)	100(2)
a (Å)	3.8735(5)	4.2914(3)	16.653(9)	3.7206(2)	6.9658(4)	5.0520(7)
b (Å)	15.890(2)	10.398(7)	13.014(6)	18.347(9)	8.0624(5)	13.194(17)
c (Å)	21.215(3)	16.176(10)	7.116(4)	10.137(5)	14.632(9)	13.292(17)
α (deg)	90	81.924(4)	90	90	75.678(4)	112.280(5)
β (deg)	92.664(6)	89.829(4)	101.118(3)	98.126(3)	81.535(4)	97.693(5)
γ (deg)	90	85.327(4)	90	90	88.527(4)	92.622(5)
Cell volume (Å^3)	1304.4(3)	712.28(8)	1513.25(14)	685.02(6)	787.50(8)	807.95(19)
Calc. density (g cm^{-3})	1.539	1.475	1.441	1.509	1.643	1.469
Z	4	2	4	2	2	2
R_{int}	0.0691	0.0368	0.0420	0.0296	0.0442	0.0388
$R_1(I > 2\sigma(I))$	0.0679	0.0475	0.05	0.0595	0.0531	0.0568
wR_2	0.2248	0.1594	0.1243	0.1987	0.1444	0.2006
Goof (S)	0.965	1.086	1.065	1.039	1.127	1.074
CCDC	1522575	1522576	1522577	1522578	1522579	1522580

Table S4. List of intermolecular H-bonding lengths and angles for five different solid forms

Crystal form	Interactions	H⋯A/Å	D⋯A/Å	<D-H⋯A/°	Symmetry code
S1	O3-H1⋯O1	2.58	3.064(4)	119	1-x,1-y,1-z
	O4-H2⋯O6	1.75	2.552(6)	164	1+x,y,z
	O6-H4⋯O5	2.56	3.233(6)	141	1/2+x,1/2-y,-1/2+z
	C15-H11⋯O2	2.53	3.455(5)	163	-x,-y,1-z
	C16-H12⋯O6	2.43	3.317(9)	154	1+x,y,z
S2	O4-H2⋯O6	1.79(3)	2.655(2)	169(2)	-x,1-y,1-z
	O6-H4⋯O3	2.11	2.922(2)	171	1+x,y,z
	C2-H5⋯O3	2.54	3.362(2)	147	-x,1-y,1-z
	C15-H9⋯O2	2.46	3.380(3)	161	1-x,2-y,-z
S3	O4-H4⋯O6	1.85	2.6686(19)	178	x,-1+y,z
	C2-H8⋯O4	2.56	3.418(2)	154	-x,-y,-z
	C4-H10⋯O6	2.53	3.211(2)	130	x,-1+y,z
	C7-H12⋯O2	2.59	3.455(2)	154	1-x,1/2+y,3/2-z
S4	O4-H2⋯N1	2.04	2.776(9)	148	1-x,1/2+y,1-z
	C17-H11⋯O2	2.46	3.227(8)	136	1+x,y,1+z
S5	O3-H1⋯O5	2.44(4)	2.980(3)	121(3)	2-x,-y,-z
	O4-H2⋯O2	2.02(4)	2.802(3)	174(5)	-x,1-y,-z
	O5-H3⋯O1	2.43(4)	2.933(3)	118(3)	2-x,-y,-z
	C4-H5⋯O2	2.54	3.242(4)	132	-x,1-y,-z
	C16-H11⋯O3	2.39	3.091(4)	128	1-x,1-y,-z
	C16-H11⋯O4	2.52	3.173(4)	124	-x,1-y,-z
S6	O3-H1⋯O5	2.55(4)	3.203(3)	133(3)	1-x,-y,-z
	O4-H2⋯O6	1.77(4)	2.671(3)	173(4)	2-x,1-y,1-z
	O5-H3⋯O1	2.41	2.876(3)	117	1-x,-y,-z

	C2-H4···O4	2.49	3.393(4)	163	3-x,-y,1-z
	C15-H10···O2	2.53	3.373(3)	147	1-x,1-y,1-z
	C18-H15···O6	2.46	3.287(7)	143	-1+x,y,z
	C16-H16B···O3	2.42	3.371(6)	165	x,1+y,z
	C19-H17···O2	2.39	3.328(6)	163	1-x,1-y,1-z
	C17-H17B···O5	2.49	3.266(9)	137	1-x,1-y,-z

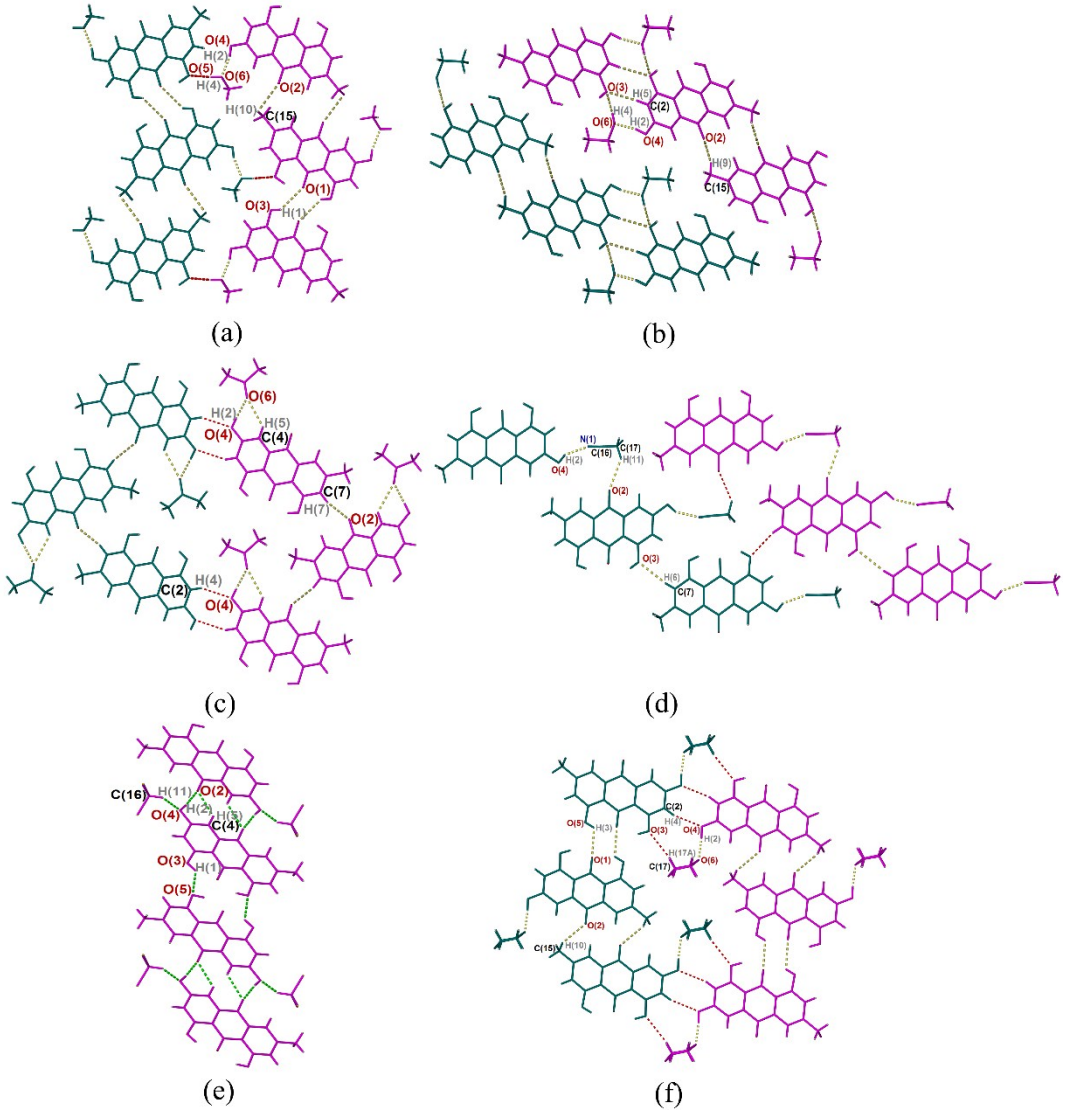

Figure S9. Single crystal H-bonding patterns of EM solvates (a) S1 [a-axis], (b) S2 [a-axis], (c) S3 [c-axis], (d) S4 [a-axis], (e) S5 [b-axis], (f) S6 [a-axis]